ARTICLE

Tunable Refractive Index Sensor with Ultracompact Structure Twisted by Poly(trimethylene terephthalate) Nanowires

Heng Zhu, Yuqing Wang, and Baojun Li*

State Key Laboratory of Optoelectronic Materials and Technologies, School of Physics and Engineering, Sun Yat-Sen University, Guangzhou 510275, China

ABSTRACT We report a tunable refractive index sensor with ultracompact structure in a 2 × 2 poly(trimethylene terephthalate) (PTT) nanowire coupling splitter assembled by twisting two flexible PTT nanowires. The sensor consists of two input branches, a twisted coupling region, and two output branches. The changes of optical power caused due to variations in the surrounding medium around the twisted coupling region were measured in the output branches. The highest measured sensitivity of the sensor is 26.96 mW/RIU (refractive index unit) and the maximum detection limit on refractive index change is 1.85×10^{-7}. The average tunabilities observed are 1.2 mW per RIU per twisted turn and 1.8 mW per RIU per 5° branching angle change.

KEYWORDS: nanowires · polymer · refractive index sensor · tunable sensor · nanophotonics

Refractive index is a very important parameter in physical, chemical, and biological applications. Such applications require accurate detection of refractive index variations to have accurate outcomes. To detect the refractive index change of an environmental medium, fiber-based refractive index sensors in a microfiber coil resonator,[1] a fiber-optic coupler,[2,3] a tapered optical fiber,[4,5] a fiber long-period grating,[6,7] and a fiber Bragg grating[8−10] have been reported. These devices have made significant contributions to refractive index sensing, but their size is usually in centimeters which limits their usage in some applications in which small size sensors are required. Because of their large surface-to-volume ratio and small diameter, nanowires are promising elements in further reducing the size of sensors and improving sensor sensitivity. Recently, a series of nanosensors in semiconductor material nanowires (*e.g.*, SnO_2, In_2O_3, ZnO, CuO, CdTe, silicon),[11−18] and carbon nanowire[19] have been reported. As one of the promising materials, polymer nanowires are also used for humidity and gas sensing.[20,21] Simulations have demonstrated that the strong evanescent field around the surface of the nanowire may be possible for refractive index sensing when a coated all-coupling nanowire microcoil resonator is used.[22] The reported refractive index detection limit of the sensor was 10^{-7}. More recently, we have demonstrated a poly(trimethylene terephthalate) (PTT) nanowire using a direct drawing method.[23] A series of ultracompact photonic coupling splitters were assembled by twisting the PTT nanowires with low insertion loss and tunable splitting ratio.[24] This motivated us to assemble a nanowire-based tunable refractive index sensor. Therefore, in this work, we report an assembly of a tunable and ultracompact 2 × 2 coupling splitter by twisting two PTT nanowires and its application in refractive index sensing.

The sensor consists of two input branches, a twisted coupling region, and two output branches, which were assembled by a simple twisting method with microstage supports under a microscope (see Methods). The nanowires used here were drawn from the PTT melt by a one-step direct drawing process.[23] Figure 1a−c shows the assembly process of the sensor. Figure 1d shows a scanning electron microscopy (SEM) image of the 2 × 2 coupling sensor with four twisted turns in the coupling region (twisted region). The diameter of the PTT nanowires used is 440 nm and the coupling region (inset of Figure 1d) is about 23 μm long and 880 nm wide. Both the input and output branching angles α and β are 20°.

For sensing applications, the twisted region (used as the sensing area) was immersed in various sample solutions with differing refractive indices. Then, the output

*Address correspondence to stslbj@mail.sysu.edu.cn.

Received for review April 16, 2009 and accepted September 7, 2009.

Published online September 11, 2009. 10.1021/nn900635b CCC: $40.75

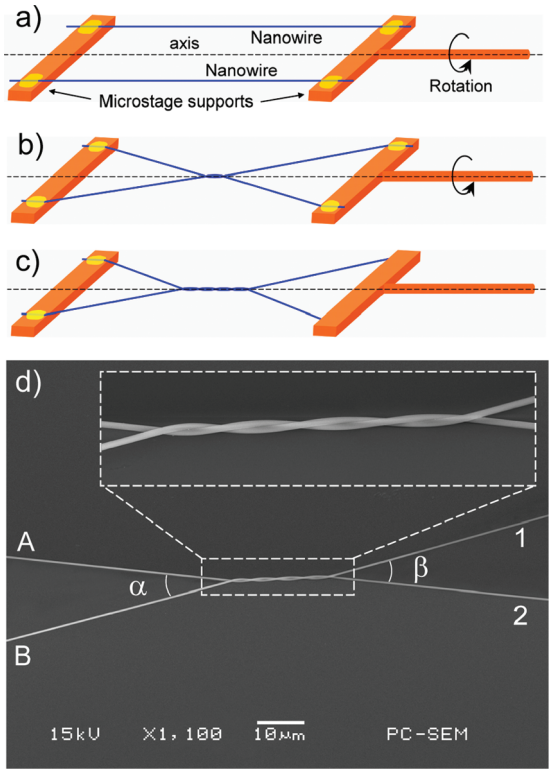

Figure 1. Fabrication process of the PTT nanowire-based tunable refractive index sensor. (a) Two parallel PTT nanowires were fixed by two microstage supports. The left support was fixed and the right support can be rotated around the axis. (b) A twisted 2 × 2 coupling sensor with one twisted turn was formed by rotating the right support. (c) A twisted 2 × 2 coupling sensor with four twisted turns was formed by further rotating the right support. (d) SEM image of the 2 × 2 coupling sensor, which was assembled by twisting two 440-nm-diameter PTT nanowires. The inset shows the twisted region with four twisted turns. The branching angles α and β are 20°.

optical signals delivered through tapered fibers get detected by optical detector and fed to power meter (see Supporting Information, Figure S1). In our characterization, sodium chloride aqueous solutions with different mass concentrations (different refractive indices of surrounding mediums) were chosen as sample solutions. Each solution droplet was dropped on the sensing area of the sensor using a microinjector (see Supporting Information, Figure S2). After each measurement, the sensor was cleaned with purified water, dried, and then prepared for different concentration solution use. In the experiment, nine sodium chloride aqueous solutions (1%, 3%, 5%, 7%, 9%, 10%, 12%, 13% and 15%) having refractive indices of 1.3387, 1.3424, 1.3462, 1.3499, 1.3536, 1.3554, 1.3591, 1.3610, 1.3647 for blue light (λ = 473 nm), 1.3358, 1.3395, 1.3431, 1.3468, 1.3504, 1.3522, 1.3559, 1.3577, 1.3613 for green light (λ = 532 nm), 1.3321, 1.3357, 1.3393, 1.3428, 1.3464, 1.3476, 1.3517, 1.3535, 1.3565 for red light (λ = 650 nm), respectively, were used. The refractive indices of the solutions were measured at room temperature using a multiwavelength Abbe refractometer, showing that

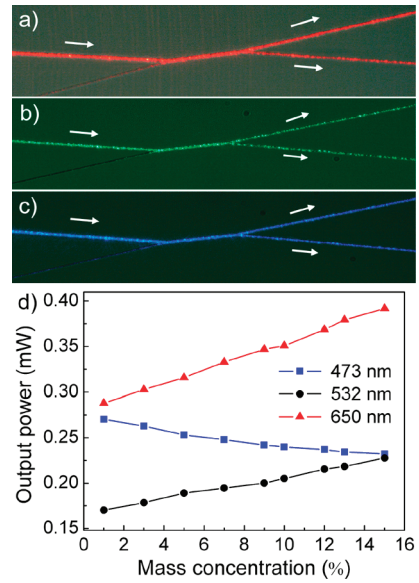

Figure 2. Optical microscopy images of the sensor taken with (a) red light (λ = 650 nm), (b) green light (λ = 532 nm), and (c) blue light (λ = 473 nm) (without sample solution). The white arrows show the propagation directions of the light. (d) Output power in the output branch 1 as a function of mass concentration of solution at branching angles of 20° and light of different wavelengths (473, 532, and 650 nm).

the refractive index depends linearly on the mass concentration.

Figure 2 panels a−c show optical microscopy images of red, green, and blue light propagated in the sensor (without sample solution), respectively. The three wavelengths were illuminated individually. The output power splitting ratios are 70:30, 50:50, and 55:45, for the red, green, and blue light, respectively. Figure 2d shows the measured power (P_1) in the output branch 1 as a function of the mass concentration of the solution at a branching angle of 20° for wavelengths of 473, 532, and 650 nm. As is evident from the results, the output power is approximately linearly related to the mass concentration. Therefore, there is a direct relationship between the output power and refractive index. In reverse, one can get to know the matter of surrounding according to the changes of the output power. The sensitivity S of the sensor is defined as $S = |\Delta P_1/\Delta n|$, where ΔP_1 is the change of the output power in the output branch 1 and Δn is the change of the refractive index of the surrounding medium. From Figure 2d, we have calculated that the sensitivities for the blue (473 nm), green (532 nm), and red (650 nm) light are 1.47, 2.19, and 4.25 mW/RIU (refractive index unit), respectively. Since the resolution of the optical power meter used is 5 nW, therefore, the detection limits of the refractive index change are about 3.40×10^{-6} (blue light), 2.28×10^{-6} (green light), and 1.18×10^{-6} (red light) for the sensor with four twisted turns in the sensing area.

The sensing mechanism of the twisted 2 × 2 coupling sensor can be explained as follows: Since the

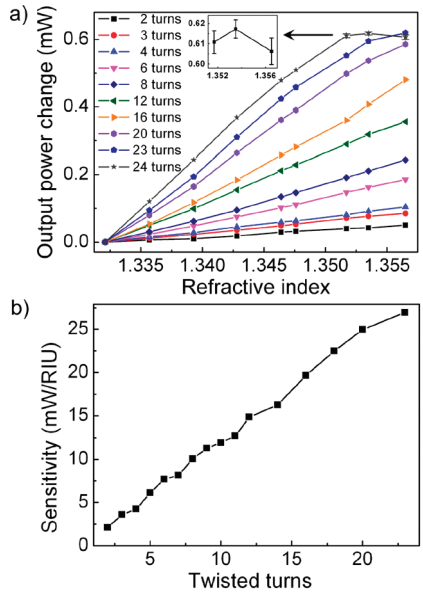

Figure 3. Twisted-turn dependence of the sensor. (a) Output power change in the output branch 1 as a function of refractive index at 650 nm wavelength with respect to the number of different twisted turns. The diameter of the nanowire is 440 nm and the input/output branching angles are around 20°. The inset shows the error bars of the output power for 24 turns with a refractive index larger than 1.35. (b) The sensitivity of the sensor *versus* the twisted turns.

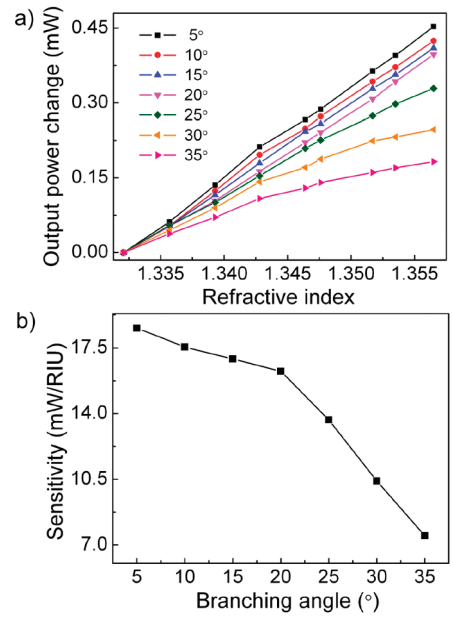

Figure 4. Input/output branching angle dependence of the sensor. (a) Output power change in the output branch 1 as a function of refractive index at 650 nm red light with different branching angles and 14 twisted turns. Input/output branching angles change from 5° to 35° with a step of 5°. (b) The sensitivity of the sensor *versus* the branching angles.

structure was assembled from nanometer-scale PTT wires, the illuminated light will be guided along the nanowires as strong evanescent waves. The change of the refractive index in the surrounding medium results in the change of the mode profile. As a result, the optical coupling property between the two nanowires in the sensing area (twisted region or coupling region) will be different and the optical power in the output branches will be changed.

To investigate the influence of the twisted turns on the sensing properties of the 2 × 2 coupling sensor, the number of twisted turns was changed by rotating the right support (Figure S1). Figure S3 in the Supporting Information shows the optical microscopy images of the sensors with different twisted turns. Figure 3a shows the measured output power change in the output branch 1 as a function of the refractive index at different twisted turns (2, 3, 4, 6, 8, 12, 16, 20, 23, and 24 turns). The wavelength of probe light used was 650 nm. Additional measured results with other twisted turns are shown in Figure S4 (Supporting Information). The change of the angles α and β caused by the change of the twisted turns is disregarded here. In the experiments, a longer coupling region causes a larger output power change for the same refractive index change. As a result, the sensitivity increases with the increase in the number of twisted turns. The sensitivity will reach a maximum value when the number of twisted turns reach a particular value. In the case of a continuous increase in the number of twisted turns, the output power in the output branch will no longer be a monotone function of the refractive index and will not be able to decide the refractive index of the surrounding medium according to the output power. In our experiment, the refractive index varies from 1.3321 to 1.3565 for red light, and the sensitivity reaches a maximum when the twisted turns is 23. Figure 3b shows the sensitivity *versus* the number of twisted turns. The calculated highest sensitivity is about 26.96 mW/RIU. In this scenario, the calculated detection limit on the refractive index change is about 1.85×10^{-7} and the measured tunability is 1.2 mW per RIU per twisted turn.

To investigate the tunability and/or branching angle dependence of the sensor, each branch end of the 2 × 2 sensor was removed from the microstage supports and then refixed to four tunable microstage supports by the PTT melt, as shown schematically in Figure S5. Since the sensitivity of the sensor increases with the number of twisted turns and reaches a maximum value at 23 twisted turns, we chose a twisted turn number less than 23 to investigate the branching angle dependence. As an example, we rotated the sensor to 14 twisted turns and fixed the sensor on the tunable microstage supports as shown in Figure S5. It should be pointed out that the branching angles of the sensor are changeable by adjusting the tunable microstage supports. The input/output branching angles α and β were changed from 5° to 35° with a step of 5° by moving the tunable microstages. Figure 4a shows the measured output power change in the output branch 1 with different branching angles at 650 nm wavelength. The measured tunability is 1.8 mW per RIU per 5°

branching angle change. The experimental results show that the sensitivity becomes higher with smaller angles of α and β, which is shown in Figure 4b. This can be explained by the fact that the effective coupling length decreases when the branching angle increases, which results in a decrease of the sensitivity. Another reason is that the bending loss in the branching region increases when the branching angle increases, leading to a decrease of the change amplitude of the output power for the same refractive index change, which will lower sensitivity.

The length of the sensing area (twisted region) fabricated here is from 12 μm (for 2 twisted turns) to 130 μm (for 23 twisted turns). The width of the sensing area (twisted region) is 880 nm (two nanowires). The maximum total length of the sensor including the input/output branches is about 4 mm. The measurement range of the sensor is about 1.332 to 1.357 in refractive index for two turns. For a sensor with 23 twisted turns, the measurement range is about 1.332 to 1.356, while for a sensor with 24 twisted turns the measurement range is 1.332 to 1.354 in refractive index. The maximum detection limit of the refractive index change of the tunable sensor is about 1.85×10^{-7} (23 turns), which is comparable with the value of $\sim 10^{-7}$ reported in ref 6 and better than those reported in ref 3 (4×10^{-6}), ref 4 ($\sim 5 \times 10^{-4}$), ref 5 (5.1×10^{-4}), and ref 9 (1.4×10^{-5}). The twist method used in assembling the sensing device is easy, cheap, and fast while avoiding the use of top-down lithography or fiber fusion technology.

In summary, an ultracompact, highly sensitive and tunable refractive index sensor has been assembled by twisting two flexible PTT nanowires. The sensor consists of two input branches, a twisted coupling region, and two output branches. The changes of optical power caused by variations in surrounding medium around the twisted coupling region were measured in the output branches. The highest sensitivity of the sensor with 23 twisted turns at 650 nm red light is 26.96 mW/RIU and the refractive index detection limit is 1.85×10^{-7}, while the sensing area is about 130 μm long and 880 nm wide. The properties of the sensor can be tuned by changing the input/output branching angles or the number of twisted turns. The average tunability per twisted turn is 1.2 mW per RIU and 1.8 mW per RIU per 5° branching angle change. The ultracompact, highly sensitive, and tunable refractive index sensor would be useful in physics, biology, biochemistry, environmental science, and toxicant sensing, while the easy, cheap, and fast twist technology would be promising in fabricating multiterminal nanosensors.

METHODS

Fabrication of PTT Nanowires. The nanowires used to assemble the sensor were drawn by a one-step process from the PTT melt. The PTT pellets (molecular weight $M_w = 35000\ g \cdot mol^{-1}$) were heated with a heating plate during the drawing. The temperature of the heating plate was kept at 250 °C using a temperature controller. Then, a silica tip was dipped into the PTT melt and then retracted with a speed of 0.1−1 m/s. Finally, a PTT nanowire was formed between the molten PTT and the silica tip.

Assembly of Sensor. The sensor was assembled by the twisting method as follows: First, a nanowire was drawn from the PTT melt by a one-step direct drawing process and then it was cut into two segments. Second, the two segment nanowires were placed in parallel on two microstage supports with their ends fixed (Figure 1a). Third, we rotated the right support in an anticlockwise direction with high precision while keeping the left support fixed (Figure 1b). The rotation was stopped when a desirable number of turns was obtained in the twisted region (*e.g.*, four twisted turns, Figure 1c). Finally, a twisted 2×2 coupling sensor was formed.

Acknowledgment. This work was supported by the National Natural Science Foundation of China (Grant 60625404). The authors thank Professor Bharat Chaudhari from the School of Information Technology, International Institute of Information Technology, Pune, India, for his assistance in the manuscript preparation and Dr. Xiaobo Xing for her fruitful discussion and assistance on the temperature dependence of nanowires.

Supporting Information Available: Schematic diagram of the sensor for characterization of the sample solution added dropwise on the sensing area of the sensor, optical microscopy images of the sensors with different twisted turns, experimental results of the sensor with twisted turns of 5, 7, 9, 10, 11, 14, and 18, and schematic diagram of the sensor for tunable characterization. This material is available free of charge *via* the Internet at http://pubs.acs.org.

REFERENCES AND NOTES

1. Xu, F.; Brambilla, G. Demonstration of a Refractometric Sensor Based on Optical Microfiber Coil Resonator. *Appl. Phys. Lett.* **2008**, *92*, 101126.
2. Smela, E.; Santlago-Aviles, J. J. A Versatile Twisted Optical Fiber Sensor. *Sens. Actuators* **1988**, *13*, 117–129.
3. Tazawa, H.; Kanie, T.; Katayama, M. Fiber-Optic Coupler Based Refractive Index Sensor and Its Application to Biosensing. *Appl. Phys. Lett.* **2007**, *91*, 113901.
4. Polynkin, P.; Polynkin, A.; Peyghambarian, N.; Mansuripur, M. Evanescent Field-Based Optical Fiber Sensing Device for Measuring the Refractive Index of Liquids in Microfluidic Channels. *Opt. Lett.* **2005**, *30*, 1273–1275.
5. Tian, Z.; Yam, S. S.-H.; Loock, H.-P. Refractive Index Sensor Based on an Abrupt Taper Michelson Interferometer in a Single-Mode Fiber. *Opt. Lett.* **2008**, *33*, 1105–1107.
6. He, Z.; Zhu, Y.; Du, H. Long-Period Gratings Inscribed in Air- and Water-Filled Photonic Crystal Fiber for Refractometric Sensing of Aqueous Solution. *Appl. Phys. Lett.* **2008**, *92*, 044105.
7. Kim, D. W.; Shen, F.; Chen, X.; Wang, A. Simultaneous Measurement of Refractive Index and Temperature Based on a Reflection-Mode Long-Period Grating and an Intrinsic Fabry-Perot Interferometer Sensor. *Opt. Lett.* **2005**, *30*, 3000–3002.
8. Chen, N.; Yun, B.; Cui, Y. Cladding Mode Resonances of Etch-Eroded Fiber Bragg Grating for Ambient Refractive Index Sensing. *Appl. Phys. Lett.* **2006**, *88*, 133902.
9. Liang, W.; Huang, Y.; Xu, Y.; Lee, R. K.; Yariv, A. Highly Sensitive Fiber Bragg Grating Refractive Index Sensors. *Appl. Phys. Lett.* **2005**, *86*, 151122.
10. Shu, X.; Gwandu, B. A. L.; Liu, Y.; Zhang, L.; Bennion, I. Sampled Fiber Bragg Grating for Simultaneous Refractive-Index and Temperature Measurement. *Opt. Lett.* **2001**, *26*, 774–776.

11. Sirbuly, D. J.; Tao, A.; Law, M.; Fan, R.; Yang, P. Multifunctional Nanowire Evanescent Wave Optical Sensors. *Adv. Mater.* **2007**, *19*, 61–66.
12. Kuang, Q.; Lao, C.; Wang, Z. L.; Xie, Z.; Zheng, L. High-Sensitivity Humidity Sensor Based on a Single SnO_2 Nanowire. *J. Am. Chem. Soc.* **2007**, *129*, 6070–6071.
13. Zhang, D.; Liu, Z.; Li, C.; Tang, T.; Liu, X.; Han, S.; Lei, B.; Zhou, C. Detection of NO_2 down to ppb Levels Using Individual and Multiple In_2O_3 Nanowire Devices. *Nano Lett.* **2004**, *4*, 1919–1924.
14. Ra, H.-W.; Choi, K.-S.; Kim, J.-H.; Hahn, Y.-B.; Im, Y.-H. Fabrication of ZnO Nanowires Using Nanoscale Spacer Lithography for Gas Sensors. *Small* **2008**, *4*, 1105–1109.
15. Chen, J.; Wang, K.; Hartman, L.; Zhou, W. H_2S Detection by Vertically Aligned CuO Nanowire Array Sensors. *J. Phys. Chem. C* **2008**, *112*, 16017–16021.
16. Mcalpine, M. C.; Ahmad, H.; Wang, D.; Heath, J. R. Highly Ordered Nanowire Arrays on Plastic Substrates for Ultrasensitive Flexible Chemical Sensors. *Nat. Mater.* **2007**, *6*, 379–384.
17. Wang, X.; Ozkan, C. S. Multisegment Nanowire Sensors for the Detection of DNA Molecules. *Nano Lett.* **2008**, *8*, 398–404.
18. Cui, Y.; Wei, Q.; Park, H.; Lieber, C. M. Nanowire Nanosensors for Highly Sensitive and Selective Detection of Biological and Chemical Species. *Science* **2001**, *293*, 1289–1292.
19. Zaitsev, A. M.; Levine, A. M.; Zaidi, S. H. Carbon Nanowire-Based Temperature Sensor. *Phys. Stat. Sol. (a)* **2007**, *204*, 3574–3579.
20. Gu, F.; Zhang, L.; Yin, X.; Tong, L. Polymer Single-Nanowire Optical Sensors. *Nano Lett.* **2008**, *8*, 2757–2761.
21. Liu, H.; Kameoka, J.; Czaplewski, D. A.; Craighead, H. G. Polymeric Nanowire Chemical Sensor. *Nano Lett.* **2004**, *4*, 671–675.
22. Xu, F.; Horak, P.; Brambilla, G. Optical Microfiber Coil Resonator Refractometric Sensor. *Opt. Express* **2007**, *15*, 7888–7893.
23. Xing, X. B.; Wang, Y. Q.; Li, B. J. Nanofiber Drawing and Nanodevice Assembly in Poly(trimethylene terephthalate). *Opt. Express* **2008**, *16*, 10815–10822.
24. Xing, X. B.; Zhu, H.; Wang, Y. Q.; Li, B. J. Ultracompact Photonic Coupling Splitters Twisted by PTT Nanowires. *Nano Lett.* **2008**, *8*, 2839–2843.